PLASMA PHENOMENA ASSOCIATED WITH SOLAR ARRAY DISCHARGES AND THEIR ROLE IN SCALING COUPON TEST RESULTS TO A FULL PANEL

Philip Leung
Michael Bodeau
The Boeing Company
Boeing Satellite System
El Segundo, California

Abstract

On a solar array, different surface potential profiles could be developed under different environmental and spacecraft operation configurations. These potential profiles were simulated in the laboratory with solar cell coupons, and the resulting discharge phenomena were investigated. The results indicated that the propagation time of the discharge generated plasma between the discharge site and the edge of the test coupon is the critical parameter in determining the waveform of the discharge current.

Introduction

Within the last few years, several solar array test programs were conducted by Boeing Satellite System (BSS) to address issues related to solar array discharges. This paper will discuss some of the results. The focus will be on the plasma phenomena associated with solar-array discharges in the GEO environment. Our research indicated that an understanding the plasma phenomena associated with discharges is extremely important as they provide clues on how to scale the coupon test results to a full flight solar panel.

The potential profile resulting from the charging of a solar array by the energetic electrons during a substorm is dependent on the spacecraft configuration and on the condition of coverglasses. Under standard operation conditions[1], unless there are large photo-emission surfaces, a spacecraft (S/C) is usually charged to a negative potential with respect to the space plasma. The coverglasses on the solar cells are exposed to sunlight, photo-electron emission from coverglasses tend to keep the their potentials less negative than the S/C structure (Figure 1). The resulting potential profile is the so call "inverted gradient" potential profile[2]. In many applications, a MgF_2 anti-reflective coating is deposited on the coverglass. MgF_2 has a very high secondary yield[3]. Even in the absence of sunlight, the secondary yield from MgF_2 coating is sufficient to maintain the inverted gradient potential profile. Therefore, for MgF_2 coated coverglass, the charging of solar array will usually result in the "inverted gradient" potential profile even during eclipse and during the time that the coverglasses are shadowed.

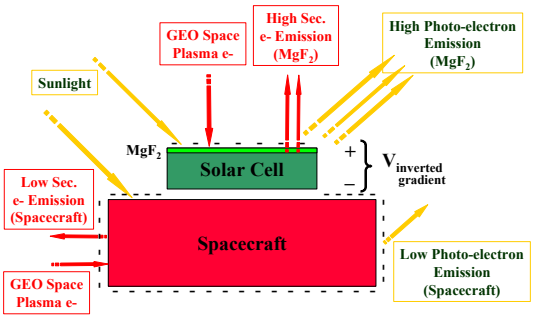

Figure 1. Inverted gradient potential profile

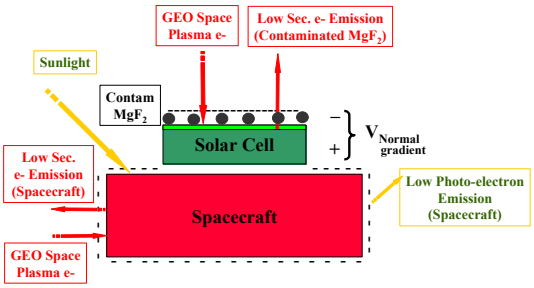

Figure 2. Normal gradient potential profile

For coverglasses without MgF_2 coating, or coverglasses that are contaminated (such that the secondary yield is dominated by contaminants), they will be charged to a more negative potential with respect to the spacecraft structure by substorm electrons when they are not exposed to sunlight. The resulting potential profile is the so-called normal gradient configuration (Figure 2).

Inverted Gradient Discharges

Laboratory simulation of the inverted gradient potential profile

In order to simulate the space environment, tests need to be conducted in a vacuum chamber. Since most test facilities are not large enough to accommodate a full solar panel, the satellite industry usually uses coupons, constructed to flight specifications, as test articles. Usually, coupons of different sizes were used so results could be scaled to a full panel. The larger the coupon, the better the accuracy is the scaling to the flight size. Figure 3 shows a picture of a large coupon used in one of our test programs.

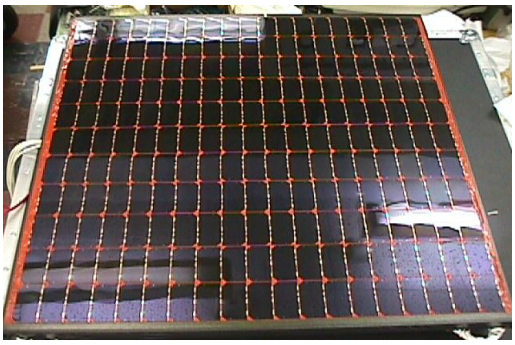

Figure 3. A large solar cell coupon. This coupon has 12x19 cells.

The inverted gradient potential profile can be simulated in the laboratory easily by the high voltage bias method[2,4,5]. Usually, a negative high voltage bias is applied to the structure, simulating the charging of the structure by the electrons. To create positively charge coverglass surfaces, the coverglasses are irradiated by electron beam or by an ultra-violet light source. In the electron beam method, the electron beam energy is selected such that the energy of electrons arriving at the coverglasses is ~ 1 KeV (for example, the electron beam energy is selected to be 3 KeV for a bias of –2 kV). For most materials[6], including coverglass materials, the secondary yield at 1 KeV is higher than 1. As a result, the coverglasses are charged to a positive potential with respect to structure, forming the inverted gradient potential profile. Figure 4 is a schematic of the high voltage biasing circuitry. In Figure 4, C_s is the capacitance of the coupon (127 pF for the coupon shown in Figure 3) with respect to chamber. A large panel/spacecraft has a capacitance of ~500 pF with respect to the space plasma. For tests to simulate the discharge from the structure of a large spacecraft, an external capacitor with a capacitance of 500 pF was placed in parallel with C_s.

In a typical test, various diagnostic instruments are used to monitor the charging and the discharging phenomena. A non-contacting voltage probe (Trek-probe) is usually used to measure the surface potential of coverglasses. Since the structure potential is at the biased voltage, this surface potential measurement provides a direct measurement of the potential difference (ΔV) between coverglasses and solar cells. Current probes, inserted at different locations of the coupon (Figure 4), are used to monitor the magnitude and the direction of the discharge current. Langmuir probes are used to detect the charge particles released in a discharge event. Figure 5 shows the arrangement of these diagnostic instruments for a typical test.

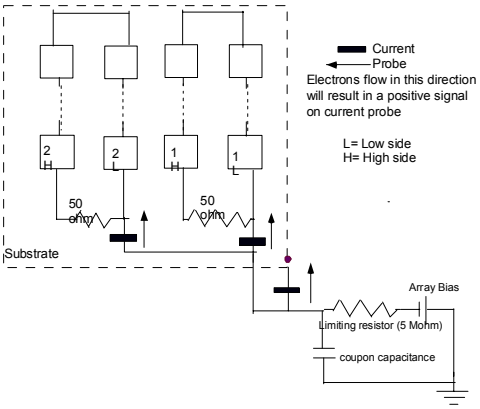

Figure 4. Schematics to simulate the inverted gradient potential profile.

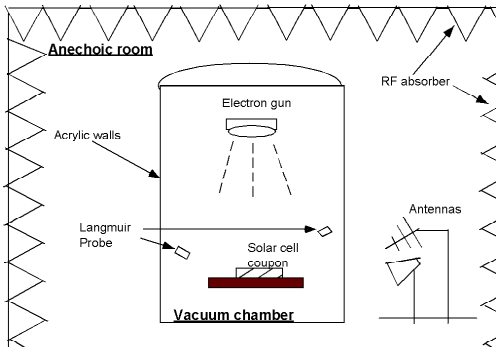

Figure 5. Diagnostic instruments.

Inverted Gradient Discharges and the Associated Plasma Phenomena

A typical example of an IG potential profile is shown in Figure 6. To create this potential profile, the structure was biased to –8 kV and the coupon was irradiated by electron beam with an energy of 9 KeV. A potential difference (ΔV) of 3 kV was developed between coverglasses and the solar cells (solar cell was at the structure potential). This ΔV was near the threshold of a discharge for this coupon, and discharges were observed. The potential profile of the coupon immediately after the discharge was also shown in Figure 6. These potential profiles indicated that the excess positive charges on the surface of the coupon were neutralized during the discharge event. The signal detected by a Langmuir Probe (LP), located at 1 meter from the coupon, was negative in sign (Figure 7) indicating electrons were emitted by the coupon during this discharge event. The coupon structure was at a potential of -8 kV with respect to ground. The electrons emitted must have energy of 8 KeV. Within the time resolution of the scope settings (~20 ns), the time delay between the onset of the discharge and the arrival of electrons was negligible, which provided another evidence that the electrons detected by LP are fast with energy of order of 5-10 keV.

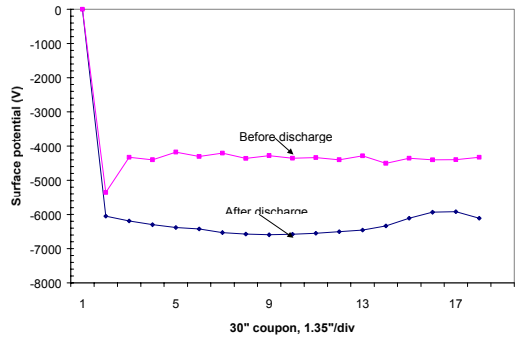

Figure 6. A typical inverted gradient potential profile. The structure was biased at –8 kV.

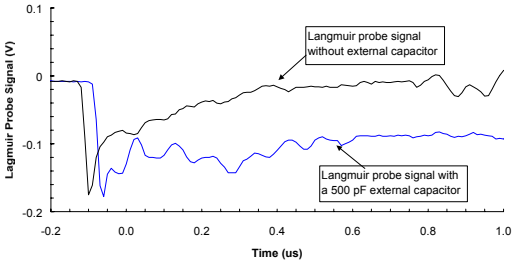

Figure 7. Langmuir probe signals.

Tests were also performed by adding a 500 pF capacitor in parallel with the existing coupon capacitance. The 500 pF capacitor was to simulate the structure capacitance of a spacecraft with large solar panels. With this external capacitor, the total capacitance was approximately 625 pF and was 5 times the capacitance of the coupon. The LP data for an IG discharge event with this external capacitor is also displayed in Figure 7. The LP data indicated that the duration of the electron pulse emitted by the coupon was 2 μs and was approximately 5 times the width without the external capacitor. The results showed that the charges stored in the structure capacitor provided the charges for the emitted electrons. The discharge current waveforms measured with and without the external capacitor are shown in Figures 8 and 9, respectively. The data show that the pulse widths were approximately equal for both waveforms, indicating that the structure capacitance did not play a role in the duration of the discharge event. At a peak current of 4 Amp, the charges stored in the structure capacitance will be depleted in 2 μs and 0.3 μs with and without the external capacitor, respectively. Consequently, the charges stored in the structure capacitance could not account for the entire current pulse and could only account for the fast electrons observed by the LP at the beginning of the discharge event.

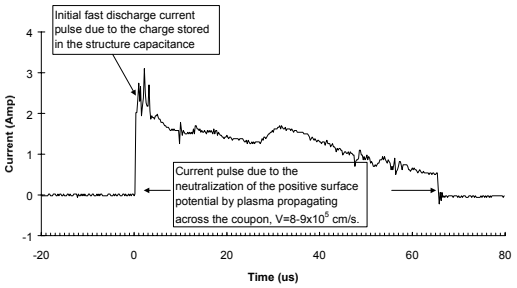

Figure 8. Inverted gradient current pulse without the external capacitor.

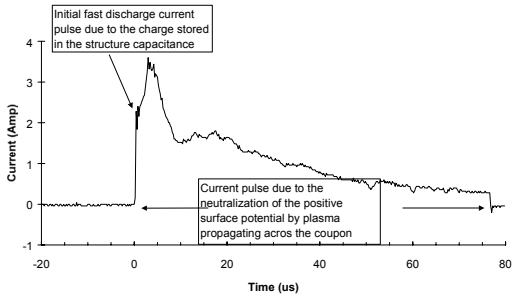

Figure 9. Inverted gradient current pulse with a 500 pF external capacitor.

Once electrons were emitted by the solar cells (at the edges or at the interconnects), they ionized the gaseous molecules in the vicinity of the solar cells producing a plasma[7]. The secondary electrons produced by ionization were attracted towards the coverglasses by the positively charged coverglasses. As a result, the secondary electrons were accelerated to energy sufficient for impact ionization producing more electrons and ions. This process kept cascading until the excess positive charges on all coverglasses were neutralized. An image of an inverted gradient discharge (Figure 10) provided evidence of this phenomenon. In this image, the bluish glow was due to excited gaseous atoms indicating the presence of a plasma. Figure 10 shows that the glow was visible throughout the entire coupon indicating the entire surface of the coupon was involved in this discharge event.

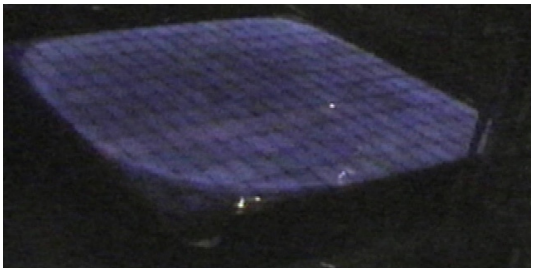

Figure 10. An image of an inverted gradient discharge.

The electron pulse detected by LP lasted for 0.4 μs (2 μs with the external capacitor). Although the duration of the discharge pulse is ~ 80 μs, the LP did not pick up any significant signal after the first couple of microseconds. The initial burst of electrons was due to the 8 keV electrons emitted by the coupon (at the solar cells or at the structure). After the charges stored in the structure capacitor were depleted, the structure potential dropped to ground potential and high-energy electrons could no longer be emitted. The plasma electrons that were responsible for neutralization of the positive charge on the coverglasses have their velocity vector pointing towards the coupon instead of away from the coupon and thus were not detected by the LP. Consequently, the high energy electron signal detected by the LP probe only lasted for microseconds.

The total charges released during an IG event can be obtained by integrating the current pulses of Figures 8 and 9. They were 84 μC for the event without the external capacitor (Figure 8) and 79 μC for the event with the external capacitor (Figure 9). The amount of charges is

much higher than the charges stored in the structure of the coupon (1 μC without the external capacitor and 6 μC with the external capacitor). For this coupon, the capacitance of each coverglass surface with respect to solar cell was 126 pF. There were 209 cells on the coupon, resulting in a total coverglass to solar cell capacitance of 0.026 μF. The potential difference between coverglasses and structure was 3.3 kV. Therefore, 87 μC (Q= CV) of charges were stored on the surface of coverglasses. This amount of charges was approximately equal to the charges released during a discharge event. Consequently, the majority (> 90%) of the charge released during an IG discharge event must originate from the coverglasses.

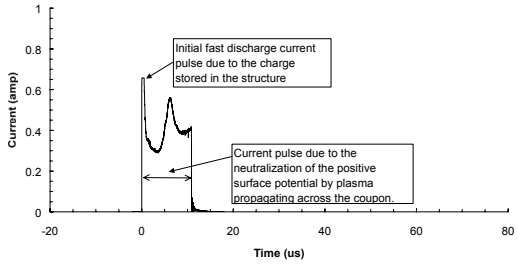

Figure 11. Inverted gradient current pulse generated by a 12" by 12" coupon.

In many applications, the scaling of the IG discharge current to a full-up solar panel is required. For this reason, tests were performed with a smaller coupon (12"x12") to determine the relevant scaling laws. A typical IG discharge current pulse obtained with the smaller coupon is shown in Figure 11. For this event, the inverted gradient potential profile was identical to the larger coupon. The structure potential was the same, i.e. at -8 kV and the ΔV between coverglasses and the solar cells was 3.3 kV. The observed pulse width of the current waveform was 12 μs. The pulse width (τ) of the ESD current pulse is related to the distance (d) between the trigger arc site and the edge of the coupon, and by the velocity of plasma (V_p) by the following relationship:

$$\tau = \frac{d}{V_p} \qquad (1).$$

Based on the dimensions of the large and small coupons, and the location of the current probes, the propagation velocities of the plasma were determined to be 8.7×10^5 cm/s and 9.5×10^5 cm/s for the large and small coupons, respectively.

Scaling to a Full Panel

For the satellite community, the major concern with IG discharges is the plasma generated by the discharge event. The plasma forms a low impedance path and could induce current to flow between cells, in particular if the cells are at a high potential with respect to each other. The current flow causes heating of the insulating substrate material and could result in a disastrous sustained short between the cells[8]. The standard industry practice is to perform tests to demonstrate new solar array designs for immunity to sustained discharge in the laboratory. In order to have a high fidelity test, the amount of plasma produces by a full panel IG discharge must be simulated properly. That is, the trigger arc[8] must produce the same amount of plasma as that of a full panel discharge. The discussions of sec. IIA and IIB provided the necessary

information to scale the IG current waveform from a coupon (and hence the plasma associated with the current pulse) to a full panel. The important points are summarized below:

1. The charges stored in the structure capacitance are responsible for the initial portion (~1 μs) of the current pulse. For the same structure capacitance, the peak current is independent of the coupon size.
2. The majority (>90%) of charges released during an IG discharge is due to the replacement current resulting from the neutralization of the charges stored on the coverglasses.
3. The width of the current pulse is proportional to the propagation time of the plasma to the edge of the coupon. For the inverted gradient condition, the plasma propagation velocity is ~$9x10^5$ cm/s.

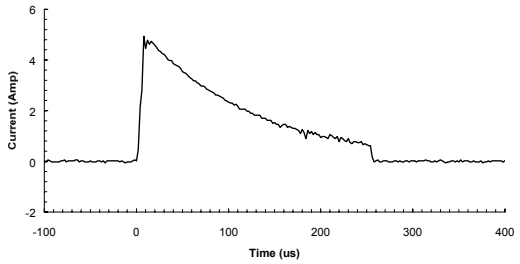

Figure 12. aveform to simulate a full panel inverted gradient discharge.

For a solar panel which has a length of 365 cm (144 in), the predicted pulse width of the discharge current is 200-400 μs. The peak current is independent of panel size. Based on the test results, the peak current is expected to be 4 Amp. Figure 12 shows a current waveform that can be used to simulate the full panel discharge.

Normal Gradient Discharges

Laboratory Simulation of the Normal Gradient Potential Profile

In the laboratory, the normal gradient (NG) potential profile is produced by irradiating the coverglasses with electron beam and with the structure of the coupon connected to chamber ground. Under this condition, the coverglasses will be charged to a negative potential with respect to the solar cells, resulting in the NG potential profile. Most of the tests[9,10] reported in literature were performed with the structure hard-grounded (i.e. grounded to chamber via a low impedance path). As the results presented in the next section shows, this method cannot simulate the space-charge phenomenon resulting from the emitted electron during a discharge event. A higher fidelity simulation method is to ground the structure of the coupon with a parallel resistor and capacitor network (Figure 13). In Figure 13, the 5 Mohm resistor isolates the structure from the chamber ground. As in the inverted gradient test, the 500 pF represents the capacitance of the spacecraft with respect to space.

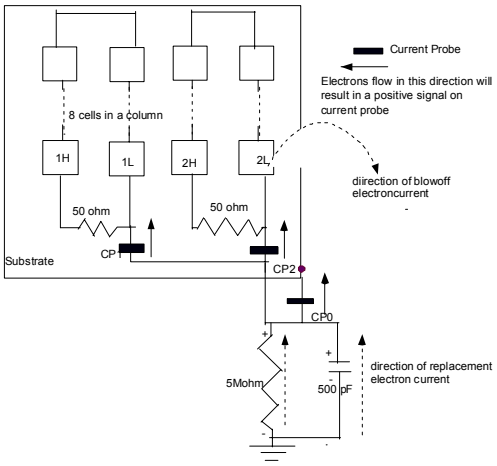

Figure 13. Normal gradient schematics with RC network grounding.

In the normal gradient test program at BSS, tests were performed with coupons of different sizes and with different cell layout configurations. One coupon had 2x4 cells (2 columns each column with 4 cells), another coupon had 4 by 8 cells (4 columns each with 8 cells). The latter coupon allowed different string configurations to be wired (1x8 and 3x8, 4x8). The different wiring configurations enabled the investigation of the scaling of ESD current with respect to cell layout configuration.

Normal Gradient Discharges and the Associated Plasma Phenomena

When the coupon was irradiated by electron beam of 22 keV, the coverglasses potential was measured to be -8 to -10 kV. Discharges were observed to occur readily. Figure 14 shows the potential profiles before and after a discharge. The data showed that >50% of the charges stored on the coverglasses were released during this discharge event. The current pulses have the waveforms shown in Figure 15. The data in Figure 15 were obtained with a 4x8 coupon wired as two 2x8 strings, and the coupon was hard-grounded. These waveforms indicated that electrons left the surface of coverglasses inducing a return current to flow in the solar cells. The peak current was measured to be 45 Amp. The pulse width was only 400 ns and was much less than the IG discharge current pulse width, indicating that NG discharge was a much faster event than IG discharge.

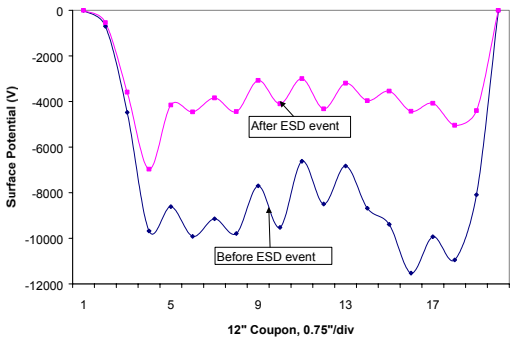

Figure 14. Normal gradient potential profiles before and after a discharge.

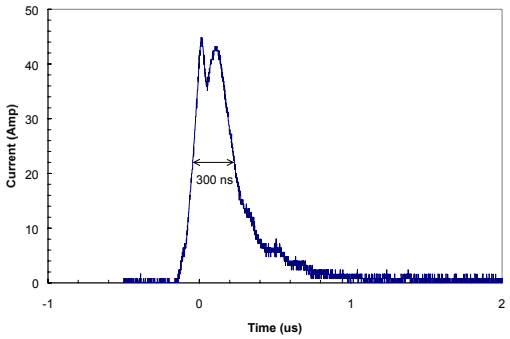

Figure 15. Normal gradient discharge current pulses

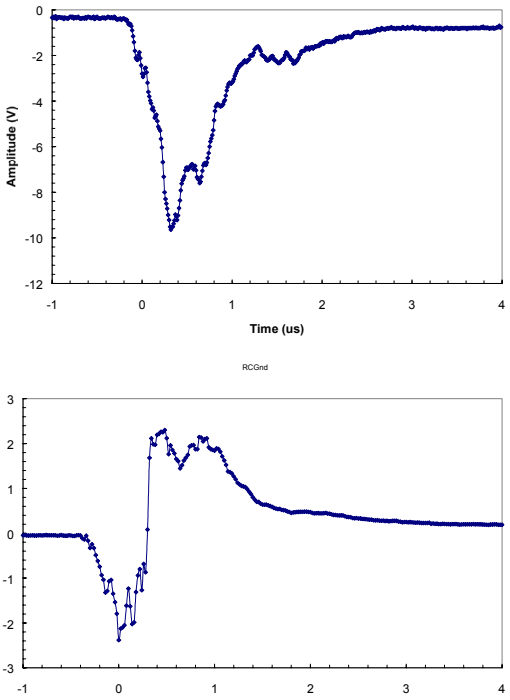

Figure 16. LP signal, NG discharge, hard-grounded (top) and via RC net work (bottom).

Tests were also conducted with the substrate grounded through the RC network. The discharge current waveforms were similar for both grounding configurations. The Langmuir probe signals, however, showed drastically different signatures (Figure 16). With the hard ground case, the LP signal was negative in sign, indicated that only electrons were collected by the LP during the NG discharge. The pulse width of LP signal was approximately equal to the width of the current pulse in the solar cell string. With the RC grounding method, the LP only collected electrons for the first 300 ns. The LP signal then turned positive indicating that ions were collected. With the RC grounding scheme, the replacement current caused the structure to charge to a positive potential (Figure 13). As a result, electrons could not escape the coupon and were forced to return to the coupon via the solar cell (interconnects or the cells) or substrate/structure. The ions produced by ionization of gaseous environment in the vicinity of the solar cells were accelerated towards the chamber ground and were collected by the LP. In space with an isolated spacecraft, a negative space charge cloud will be formed around the

vehicle during a NG discharge. The electric field due to this space charge will force the electrons back to the spacecraft just like the RC grounding case.

Discharge Current Scaling for Normal Gradient Discharge

It is important to know the magnitude of the current induced in solar cells so that the susceptibility of the solar cells to discharge current can be quantified. In an actual solar panel, there are many ways to lay out the cells. Usually, the cells are arranged in strings so that the voltage output of each string is equal to the operation voltage of the array. For typical solar cells, a 50 Volt string requires ~30 solar cells while a 100 Volt string entails ~ 60 solar cells. These cells can be arranged in a long string of 30 to 60 solar cells or they can be arranged in a serpentine fashion with each segment of serpentine containing 5-10 cells.

Tests were performed to characterize the discharge current induced in the solar cells for the long string and for the serpentine configurations. For the long string configuration, tests were conducted on coupons with 2x4 cells and 2x8 cells. The test results are shown in Figure 17. The results show that for the long string configuration, the peak current is independent of the string length. However, the pulse width increases linearly with the length of the string. These results agreed with the results of Bogorad[9]. For a long string, the time required for the plasma generated at the discharge site to propagate the long dimension (end of the string) is much longer than the time to the short dimension (edge of the coupon). Consequently, the waveform of the discharge current is dominated by the length of the string (number of cells in a string). The discharge current (I_d) is given by:

$$I_d = \frac{\Delta Q}{\Delta t} \quad (2).$$

A longer string loses more charges (ΔQ) during a discharge event. However, the time duration (Δt) of the discharge is also longer. For this reason, the peak current was observed to be independent of the number of cells in a string. From the data, the plasma propagation speed was estimated to be 3.6×10^7 cm/s. The higher speed, as compared to IG plasma propagation speed, was due to the higher ΔV in the NG (8 kV vs 3 kV).

The discharge current of the serpentine configuration was investigated by wiring the 4x8 coupon into strings of 1x8, 2x8, 3x8 and 4x8. Current probes were inserted at each string to measure the discharge current. The results are shown in Figure 18. In this figure, only the highest peak current was plotted. The objective was to compare the results to the well-established Balmain area scaling relationships[10]. Balmain's test results indicated that the peak-current increased with the square root of the area. For our test configuration, the area is proportional to the number (N) of segment in the serpentine. Therefore, the peak current should scale with $\sqrt{N}$. Figure 18 shows that the data did follow the square root relationship indicating that Balmain area scaling law is valid for solar cells coupon/panel when the dimension of width and length were of the same order of magnitude. In this configuration, the total charge released is proportional to the area of the coupon, but the plasma propagation time is proportional to the linear dimension of the coupon. Consequently, the peak current (equation 2) is proportional to the linear dimension of the coupon, i.e. square root of the area.

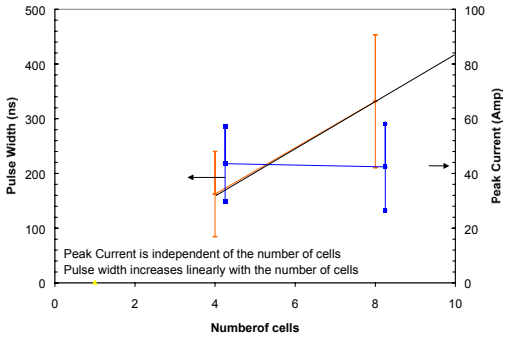

Figure 17. Peak discharge current and pulse width vs the number of cells in a string

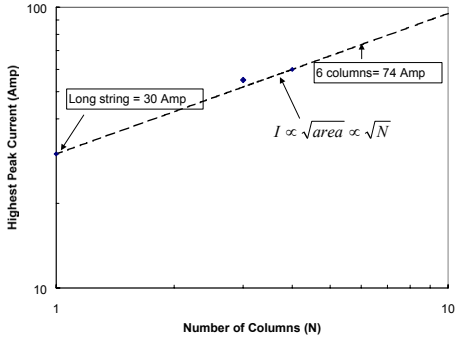

Figure 18. Peak current vs number of columns in a serpentine.

Summary

Results of laboratory simulation of solar array charging and discharging for both the inverted gradient and the normal gradient potential profiles were discussed in this paper. In an inverted gradient discharge, the initial current pulse is due to fast electrons emitted by the solar cell coupon. The fast electron emission is terminated when the charges stored in the structure capacitance of the solar array/coupon are depleted. For this reason, the peak current of a solar panel IG discharge is dependent on the structural capacitance only and is independent of the size of the solar panel. The displacement current resulting from the neutralization of the positive charge stored on the coverglasses is responsible for > 90% of the charge in the discharge current pulse. The time duration of this discharge current pulse is governed by the plasma propagation time from the discharge site to the end of the coupon, and hence scales linearly with the panel size.

In the normal gradient discharge, the discharge current waveform is again dominated by the propagation time of plasma from the site of the discharge to the edge of the coupon. The peak current of a square/rectangular segment obeys the Balmain's scaling law. That is, the peak current increases with the square root of the area. However, this scaling law is only valid for a solar panel segment where the dimensions of the length and width are of the same order of magnitude. For a long string, the peak current is independent of the number of cells in the string whereas the pulse width increases linear with the number of strings. The long string follows a modified scaling relationship as the time required for the discharge produce plasma to go from the discharge site to the edge of the solar panel is much longer in the long dimension than in the

short dimension. Consequently, the waveform of the discharge current is governed by the length of the string (number of cells in a string).

Acknowledgement

Many engineers and scientist at Boeing Satellite System contributed to this work. The authors would like to acknowledge the input from R. Parker, Joel Schwartz and J. Matossian. J. Fang , M. Wong and S. Seki helped with the test setup. Greg Tettemer provided expert assistance in data acquisition and data reduction.

References

1. Whipple,E.C., “The Equilibrium Electric Potential of a Body in the Upper Atmosphere,” NASA X-615-65-296.

2. Stevens, et al., “Voltage Gradients in Solar Array Cavities as Possible Breakdown Sites in S/C Charging Induced Discharges,” IEEE Transactions on Nuclear Science, Vol. NS-28, No. 6, Dec. 1981, pp. 4558-4562.

3. Krainshy, I., Lundin, W., Gordon, W.I., Hoffman,R.W., “Secondary Electron Emission Yield”, Case Western Reserve University Report for NASA Grant NSG 3197. September 1981.

4. Leung, P., “Discharge Characteristics of a Simulated Solar Cell Array,” IEEE Transactions on Nuclear Science, Vol. NS-30, No. 6, Dec. 1983, pp. 4311-4315.

5. Snyder, D., “Environmentally Induced Discharges in a Solar Array,” IEEE Transactions on Nuclear Science, Vol. NS-29, No. 6, Dec. 1982, pp. 1607-1609.

6. Garrett, H.B., “Spacecraft Charging: A Review”, Space Systems and Their Interactions With Earth'' Space Environment, AIAA, New York, 1980.

7. Leung, P. and Plamp G., “Characteristics of RF Resulting from Dielectric Discharges”, IEEE Transaction on Nuclear Science, December 1982, p. 1610-1614, 1982.

8. Katz, I., Davis, V., and Snyder, D., “Mechanism for Spacecraft Charging Initiated Destruction of Solar Arrays in GEO,” AIAA 36th Aerospace Sciences Meeting, Reno, Nevada, 1998.

9. Bogorad et. al., “The Effects of Conducting Breaks on Electrostatic Discharge (ESDs) on Optical Solar Reflector (OSR) Panels, IEEE NS-39, No.6, Dec 1992, p.1790-1796.

10. Balmain, K.G., “Surface Discharge Effects”, in Space Systems and Their Interactions with Earth’s Space Environment, Edited by Garrett and Pike, AIAA, New York, 1980.